

Resolving long-range spatial correlations in jammed colloidal systems using photon correlation imaging

A. Duri^{1,2}, D.A. Sessoms³, V. Trappe³, and L. Cipelletti^{1,*}

¹*LCVN, UMR 5587 Université Montpellier 2 and CNRS, France*

²*IATE, UMR 1208, INRA-CIRAD-UMII-Supagro, France*

³*Département de Physique Université de Fribourg, Suisse*

*

(Dated: October 30, 2018)

We introduce a new dynamic light scattering method, termed photon correlation imaging, which enables us to resolve the dynamics of soft matter in space and time. We demonstrate photon correlation imaging by investigating the slow dynamics of a quasi two-dimensional coarsening foam made of highly packed, deformable bubbles and a rigid gel network formed by dilute, attractive colloidal particles. We find the dynamics of both systems to be determined by intermittent rearrangement events. For the foam, the rearrangements extend over a few bubbles, but a small dynamical correlation is observed up to macroscopic length scales. For the gel, dynamical correlations extend up to the system size. These results indicate that dynamical correlations can be extremely long-ranged in jammed systems and point to the key role of mechanical properties in determining their nature.

PACS numbers: 64.70.pv,82.70.-y,82.70.Rr

The slow relaxation of molecular fluids, colloidal suspensions and granular materials becomes increasingly heterogeneous [1, 2, 3, 4, 5] as the glass [6] or jamming [7] transitions is approached. In these systems, structural relaxation occurs through the correlated motion of clusters of particles, leading to spatial correlations of the local dynamics. Simulations [3] and experiments [1, 2, 4, 8, 9] of molecular and colloidal supercooled fluids show that the range of dynamical correlations is typically moderate, extending over at most a few particles close to the glass transition. Experiments in driven granular systems [5, 10] support similar conclusions for athermal systems approaching jamming. However, it has been recently argued [11] that in jammed materials any local rearrangement should propagate elastically over larger distances, leading to long-ranged dynamical correlations.

Testing these ideas is a challenging task. Spatial correlations of the dynamics can of course be investigated in simulations, but the linear size of the simulation box is typically limited to 10-20 particles. Optical or confocal microscopy of colloidal suspensions or imaging of 2-dimensional driven granular materials could in principle address this issue. In practice, however, the number of particles that can be followed is limited. This is because the spatial resolution is a fixed fraction of the field of view in conventional imaging techniques. Near jamming, however, the particle displacements are very restrained, such that a high magnification has to be chosen to resolve them; this consequently limits the field of view and thus the number of probed particles.

Here, we overcome these limitations by introducing a novel optical method that combines features of both dynamic light scattering [12] and imaging. The method, termed Photon Correlation Imaging (PCIm) [13], decouples the length scale over which the dynamics is probed

from the size of the field of view, thereby allowing long-ranged correlations to be measured. We demonstrate PCIm by measuring the range, ξ , of spatial correlations in the dynamics of three systems: a diluted suspension of Brownian particles, and two jammed materials, a dry foam and a colloidal gel. As expected, we find no spatial correlations in the dynamics of the Brownian particles. For the foam consisting of deformable bubbles that can easily slip around each other, ξ is of the order of a few bubble sizes, but partially correlated motion is also observed on larger length scales. For the gel consisting of rigidly bound hard colloids, the range of correlation is comparable to the system size, thousands of times larger than the particle size.

The Brownian particles are polystyrene spheres of radius 265 nm, suspended in a mixture of water and glycerol at a volume fraction $\varphi \sim 10^{-4}$. The foam is a commercial shaving foam consisting of tightly packed, poly-disperse bubbles (gas fraction ≈ 0.92), a model system used to study intermittent dynamics in previous investigations [14]. To avoid multiple scattering, we confine the foam in a thin cell, of thickness 1-2 bubble layers. The foam coarsens with time: the data reported here are taken 6.1 h after producing the foam, when the average bubble radius is $\sim 80 \mu\text{m}$. As an example of a system where jamming results from attractive interactions, we study a gel made of aggregated polystyrene particles of radius 20 nm at $\varphi = 6 \times 10^{-4}$, 32.3 h after the gel was formed. Details of the system can be found in [15, 16]; its average dynamics are representative of those of a wide class of soft materials. We express all time scales in units of τ_r , the relaxation time of the average dynamics, defined by $f(\tau_r) = e^{-1}$, with $f(\tau)$ the usual average dynamic structure factor. For the Brownian particles, foam, and gel, $\tau_r = 42, 140, \text{ and } 5000 \text{ s}$, respectively. For all sam-

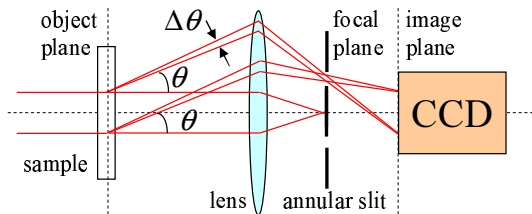


FIG. 1: (Color online) Schematic view of the low-angle, space-resolved light scattering apparatus.

ples, the dynamics are stationary on the time scale of the experiments.

A scheme of the space-resolved dynamic light scattering apparatus is shown in Fig. 1. The sample cell of thickness $L = 2$ or 0.1 mm for colloids and foams, respectively, is placed in a temperature-controlled bath (not shown) and is illuminated by a collimated laser beam with a diameter of 8 mm and a wavelength $\lambda = 633$ nm. A lens with a focal length $f_L = 40$ mm is used to form an image of the sample onto the detector of a CCD camera, typically with magnification 0.8 - 1.3 . We place an annular aperture of radius $r_a = 9$ mm in the focal plane of the lens, so that only light scattered within a small angular interval $\Delta\theta/\theta \approx 0.1$ around $\theta \approx 6.4$ deg contributes to the formation of the image. The images have a speckled appearance; each speckle receives light scattered from a small volume of lateral extension $\approx \lambda/\Delta\theta$ [17] and depth L . Our setup combines features of both imaging and scattering methods: similarly to imaging techniques and in contrast to usual scattering methods, each location on the CCD detector corresponds to a precise location in the sample. However, similarly to scattering methods and unlike conventional imaging, only light scattered at a chosen angle and thus scattering vector q is collected by the detector, allowing one to probe the dynamics of the sample on a well defined length scale $\Lambda \approx q^{-1} \approx 1 \mu\text{m}$, optimized according to the sample features.

Speckle correlography [17] and setups similar to the one in Fig. 1 [18, 19] have been used in the past to study structural properties. Here we focus on dynamical properties. We take a time series of CCD images at a fixed rate; each image is divided in regions of interest (ROIs), typically squares of side $10 - 20$ pixels containing ~ 100 speckles and corresponding to about $50^2 - 150^2 \mu\text{m}^2$ in the sample. The local dynamics within a given ROI is quantified by a two-time degree of correlation [20]:

$$c_I(t, \tau; \mathbf{r}) = \frac{\langle I_p(t)I_p(t + \tau) \rangle_{\text{ROI}(\mathbf{r})}}{\langle I_p(t) \rangle_{\text{ROI}(\mathbf{r})} \langle I_p(t + \tau) \rangle_{\text{ROI}(\mathbf{r})}} - 1, \quad (1)$$

with \mathbf{r} the position of the center of the ROI, $I_p(t)$ the intensity of the p -th pixel of the ROI at time t , and $\langle \dots \rangle_{\text{ROI}(\mathbf{r})}$ the average taken over all pixels within the ROI. The space and time resolved dynamic struc-

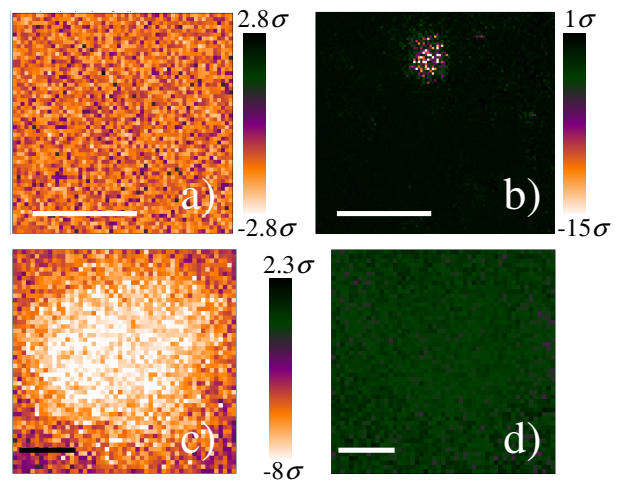


FIG. 2: (Color online) Dynamic activity maps; the bars correspond to 2 mm. The color code indicates, in units of standard deviations σ , the fluctuations of the local c_I with respect to its temporal average. a): Brownian particles ($\tau = 0.2$ s, $\tau/\tau_r = 0.0048$); b) foam ($\tau = 3$ s, $\tau/\tau_r = 0.021$); c) and d): colloidal gel ($\tau = 500$ s, $\tau/\tau_r = 0.1$) during a rearrangement event and a quiescent period, respectively.

ture factor is given by $f(t, \tau; \mathbf{r}) = \sqrt{\beta^{-1}c_I(t, \tau; \mathbf{r})}$, with $\beta \lesssim 1$ an instrumental constant [12] and $f(t, \tau; \mathbf{r}) = N^{-1} \sum_{j,k} \exp[i\mathbf{q} \cdot (\mathbf{r}_j(t) - \mathbf{r}_k(t + \tau))]$, where the sum is over the N scatterers belonging to the sample volume associated to the ROI. The usual intensity correlation function $g_2(\tau) - 1$ measured in traditional light scattering is the average of $c_I(t, \tau; \mathbf{r})$ over both t and \mathbf{r} . By applying Eq. (1) to all ROIs, we build a “dynamical activity map” (DAM) showing the local degree of correlation, characterizing the change in configuration during the time interval $[t, t + \tau]$.

In Fig. 2 we show representative DAMs for the three samples; movies displaying sequences of DAMs can be found in [21]. While previous works on dynamical heterogeneity have often dealt with the spatial correlation of the dynamics on a time scale comparable to the average relaxation time τ_r [5, 10, 22], here we focus on smaller time lags, for which individual rearrangement events are best visualized. As a control test, we show in Fig. 2a a DAM for a suspension of Brownian particles. The dynamics exhibit spatial fluctuations, without any obvious spatial correlation, consistent with the behavior expected for diluted, non-interacting scatterers. A typical DAM for the foam exhibiting an intermittent rearrangement event is shown in Fig. 2b. Contrary to the case of the Brownian particles, the dynamics is inhomogeneous: the bright spot at the top of the field of view corresponds to an extended region with a large loss of correlation, while the rest of the sample experiences only a marginal change in configuration. The DAM movie [21] reveals that the foam dynamics is dominated by similar events. We identify these intermittent, localized events with the bubble rearrangements driven by the accumulation of internal

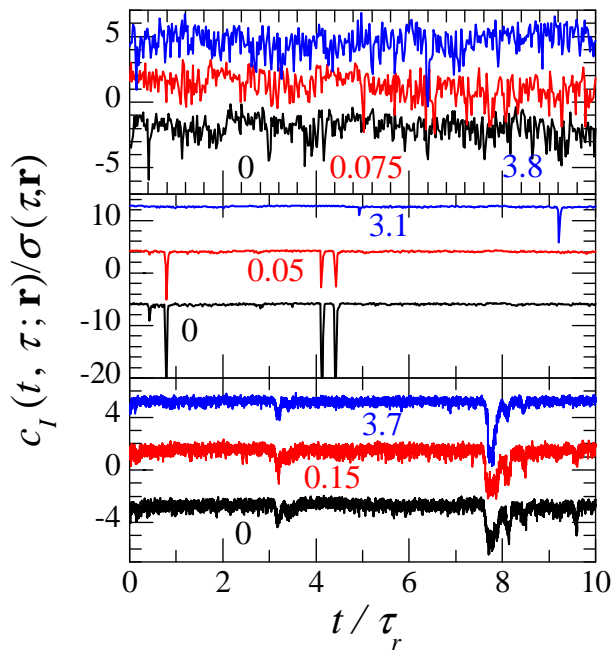


FIG. 3: (Color online) Instantaneous degree of correlation $c_I(t, \tau, \mathbf{r})$, normalized by its standard deviation $\sigma(\tau, \mathbf{r})$, measured at three different locations in the sample, as a function of reduced time t/τ_r (for the sake of clarity, the curves are offset along the vertical axis and only a limited portion of the data is shown). Data have been corrected for instrumental noise as explained in Ref. [23]. For each sample, curves are labeled by the distance in mm with respect to the location for the black curve. Top: Brownian particles (the labels 0, 0.075 and 3.8 refer to the traces from bottom to top); middle: foam; bottom: colloidal gel. For all samples, τ/τ_r is as in Fig. 2.

stress due to coarsening. Spatial maps of the dynamics of the colloidal gel are shown in Fig. 2c and d. Similarly to the foam, the dynamics is due to intermittent rearrangement events (c), separated by quiescent periods (d). These events, however, extend over strikingly large length scales, comparable to the system size, suggesting that any local rearrangement must propagate very far throughout the network.

To better evaluate the spatio-temporal correlations of the dynamics, we compare in Fig. 3 the time evolution of the instantaneous degree of correlation $c_I(t, \tau; \mathbf{r})$ in three ROIs, two of which are adjacent, while the third one is at least 3.1 mm apart from the first one. Data for the Brownian particles are shown in the top panel. The local dynamics fluctuates in a noise-like way and fluctuations in distinct ROIs appear to be uncorrelated, whatever the distance between ROIs. For the foam (middle panel), individual rearrangement events such as the one observed in Fig. 2b result in deep downward spikes, lasting ~ 3 s, departing from the average value of c_I by several standard deviations. The depth of the spikes is a measure of the displacement of the scatterers compared to Λ . The

c_I traces for adjacent ROIs appear to be strongly correlated, while the spikes in the trace of the third ROI are almost completely uncorrelated, consistently with the typical event size inferred from the DAM of Fig. 2b. For the colloidal gel (bottom panel), we find that essentially all ROIs present strongly correlated c_I traces, suggesting that the ultra-long ranged rearrangement events depicted in Fig. 2c are indeed representative of the typical behavior of the gel. Their duration is of the order of 10^3 s.

We quantify the spatial correlation of the dynamics by introducing a “four point” correlation function $\tilde{G}_4(\Delta r, \tau)$ that compares the dynamical activity in two small regions separated by Δr . We define \tilde{G}_4 as the crosscorrelation of the local dynamics [3, 5, 10, 22]:

$$\tilde{G}_4(\Delta r, \tau) = \left\langle \frac{\langle \delta c_I(t, \tau; \mathbf{r}_1) \delta c_I(t, \tau; \mathbf{r}_2) \rangle_t}{\sigma(\tau, \mathbf{r}_1) \sigma(\tau, \mathbf{r}_2)} \right\rangle_{|\mathbf{r}_1 - \mathbf{r}_2| = \Delta r}. \quad (2)$$

Here, $\delta c_I(t, \tau; \mathbf{r}) = c_I(t, \tau; \mathbf{r}) - \langle c_I(t, \tau; \mathbf{r}) \rangle_t$ and $\sigma(\tau, \mathbf{r}) = \sqrt{\langle \delta c_I(t, \tau; \mathbf{r})^2 \rangle_t}$, with $\langle \dots \rangle_t$ an average over time. Figure 4 shows \tilde{G}_4 for the Brownian particles (blue squares). The spatial correlation decays nearly completely over one ROI size, confirming that the dynamics of diluted Brownian particles are spatially uncorrelated. The spatial correlation of the dynamics of the foam and the gel are shown in Fig. 4 as orange triangles and black circles, respectively. Here, a slightly different normalization has been chosen: as discussed in Ref. [23], c_I contains a noise contribution stemming from the finite number of speckles. The noise of distinct ROIs is uncorrelated and thus does not contribute to the numerator of Eq. (2); however, it does add an extra contribution for $\Delta r = 0$, and it contributes to the σ terms in the denominator. We thus plot only data for $\Delta r > 0$ and define $G_4(\Delta r, \tau) = b \tilde{G}_4(\Delta r, \tau)$, with $b \gtrsim 1$ chosen so that $G_4(\Delta r, \tau) \rightarrow 1$ for $\Delta r \rightarrow 0$.

For the foam, most of the decay of G_4 is well described by a slightly compressed exponential, $G_4 = \exp[(-\Delta R/\xi)^p]$, with $p = 1.27$ and $\xi = 0.6$ mm (black line), corresponding to 8 bubble radii, denoting the size of rearrangement events, in agreement with previous estimates [14]. Interestingly, this decay is followed by a plateau $G_4 \approx 7 \times 10^{-2}$ that extends over the full field of view, $\Delta r \lesssim 4$ mm. This indicates that, although the spatial correlations of the dynamics are dominated by the typical size of rearrangements, the events have also a small impact on the rest of the sample. A comparison with younger foams, where the confinement is less severe, suggests that this long-range strain propagation is due to the strong confinement of the sample investigated. Elastic strain propagation has a dramatic effect in the gel, where the range of dynamical correlation is strikingly large: G_4 only decays by about 25% over 8 mm. A compressed exponential fit of G_4 (red line) yields $p = 1.8$ and $\xi = 16.4$ mm, demonstrating that the dynamics are strongly correlated over distances far larger than any relevant structural length scale: the particle

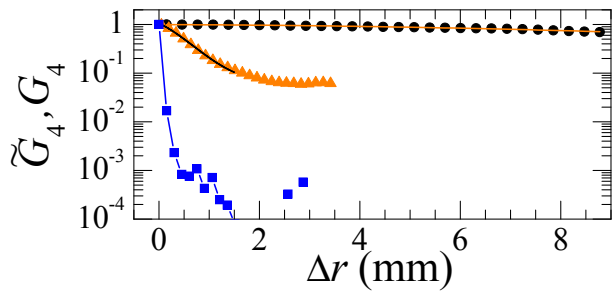


FIG. 4: (Color online) Spatial correlation of the dynamics for diluted Brownian particles (\widetilde{G}_4 , blue squares), for a foam (G_4 , orange triangles), and for a colloidal gel (G_4 , black circles). The lines are stretched exponential fits to the decay of G_4 , yielding $\xi = 0.6$ and 16.4 mm for the foam and the gel, respectively. For all samples, τ/τ_r is as in Fig. 2.

diameter is 20 nm and the gel is formed by fractal clusters of size $\approx 20 \mu\text{m}$ [15]. The differences observed in the spatial correlations of our two jammed systems can be understood considering the differences in the response to a local change of configuration. The foam consists of deformable bubbles, for which the resistance to sliding around each other is relatively small. Any local rearrangement is then mostly dissipative, involving the topological rearrangement of a few bubbles, and setting only a small elastic strain on the surrounding medium. By contrast, in the colloidal gel the rigid connection of particles to a stress-bearing backbone entails a long-ranged strain field, as both the particles and the bonds between them are rigid and do not allow for a localized reorganization.

Our experiments show that the dynamics of jammed systems can exhibit surprisingly long-ranged spatial correlations, which exceed by far those reported in previous works on molecular and colloidal glass formers and in driven granular media [1, 2, 3, 4, 5, 8, 9, 10, 22]. The technique introduced here should provide a flexible and valuable tool to characterize spatial correlations of the dynamics. PCIm-experiments can be performed in any of the classical light scattering geometries, including small angle (where Λ can be tuned by varying r_a/f_L), wide angle (see Fig. SM1 in [21]), and diffusing wave spectroscopy in the backscattering geometry [24], thereby providing access to a range of length-scales spanning more than 1.5 decades. Ongoing wide angle PCIm experiments performed on Laponite [25], closely packed onions [26], and a fibrin film [27] suggest that the long range dynamical correlations observed here for the gels may be very general. In the future, it would be interesting to compare systematically dynamical correlations in jammed (connected) systems and glassy (disconnected) systems. Finally, we stress that PCIm could also be extended to different kinds of radiation, to probe for instance molecular glass formers. Indeed, the optical layout shown Fig. 1 is similar to the one used in Fluctuation

Electron Microscopy (FEM) [28] and the PCIm method could be adopted to analyze the FEM speckle images to monitor the dynamics with spatial resolution.

This work was supported by CNES, ACI JC2076, CNRS (PICS n. 2410), and the Swiss National Science Foundation. L.C. acknowledges support from the Institut Universitaire de France.

* Electronic address: lucacip@lcvn.univ-montp2.fr

- [1] M. D. Ediger, *Annu. Rev. Phys. Chem.* **51**, 99 (2000).
- [2] R. Richert, *J. Phys.: Condens. Matter* **14**, R703 (2002).
- [3] S. C. Glotzer, *J. Non-Cryst. Solids* **274**, 342 (2000).
- [4] E. R. Weeks, J. C. Crocker, A. C. Levitt, et al., *Science* **287**, 627 (2000).
- [5] O. Dauchot, G. Marty, and G. Biroli, *Phys. Rev. Lett.* **95**, 265701 (2005).
- [6] E. Donth, *The Glass Transition* (Springer, Berlin, 2001).
- [7] A. J. Liu and S. R. Nagel, *Nature* **396**, 21 (1998).
- [8] L. Berthier, G. Biroli, J. P. Bouchaud, et al., *Science* **310**, 1797 (2005).
- [9] C. Dalle-Ferrier, C. Thibierge, C. Alba-Simionesco, et al., *Phys. Rev. E* **76**, 041510 (2007).
- [10] A. S. Keys, A. R. Abate, S. C. Glotzer, and D. J. Durian, *Nature Physics* **3**, 260 (2007).
- [11] G. Picard, A. Ajdari, F. Lequeux, and L. Bocquet, *Phys. Rev. E* **71**, 010501(R) (2005).
- [12] B. J. Berne and R. Pecora, *Dynamic Light Scattering* (Wiley, New York, 1976).
- [13] A. Duri, PhD Thesis, Université Montpellier 2 (2006).
- [14] D. J. Durian, D. J. Pine, and D. A. Weitz, *Science* **252**, 686 (1991).
- [15] L. Cipelletti, S. Manley, R. C. Ball, and D. A. Weitz, *Phys. Rev. Lett.* **84**, 2275 (2000).
- [16] A. Duri and L. Cipelletti, *Europhys. Lett.* **76**, 972 (2006).
- [17] J. W. Goodman, *Speckle phenomena in optics: theory and applications* (Roberts & Co., Englewood, 2007).
- [18] D. B. Williams and C. B. Carter, *Transmission Electron Microscopy: A Textbook for Materials Science* (Plenum, New York, 1996).
- [19] H. J. Schope, A. B. Fontecha, H. König, J. M. Hueso, and R. Biehl, *Langmuir* **22**, 1828 (2006).
- [20] L. Cipelletti, H. Bissig, V. Trappe, et al., *J. Phys.: Condens. Matter* **15**, S257 (2003).
- [21] Supplementary Online Material.
- [22] N. Lacevič, F. W. Starr, T. B. Schroder, V. N. Novikov, and S. C. Glotzer, *Phys. Rev. E* **66**, 030101(R) (2002).
- [23] A. Duri, H. Bissig, V. Trappe, et al., *Phys. Rev. E* **72**, 051401 (2005).
- [24] D. A. Weitz and D. J. Pine, in *Dynamic Light scattering*, edited by W. Brown (Clarendon Press, Oxford, 1993), Vol. 652.
- [25] A. Mourchid, A. Delville, J. Lambard, E. Lecolier, and P. Levitz, *Langmuir* **11**, 1942 (1995).
- [26] L. Ramos and L. Cipelletti, *Phys. Rev. Lett.* **87**, 245503 (2001).
- [27] R. F. Doolittle, *Annu. Rev. Biochem.* **53**, 195 (1984).
- [28] J. M. Gibson and M. M. J. Treacy, *Phys. Rev. Lett.* **78**, 1074 (1997).